Available online at www.sciencedirect.com
SCIENCE DIRECT®
International Journal of Pharmaceutics 257 (2003) 195–203
international journal of pharmaceutics
www.elsevier.com/locate/ijpharm

Development of polymeric nanoparticulate drug delivery systems: evaluation of nanoparticles based on biotinylated poly(ethylene glycol) with sugar moiety

In-Sook Kim, Sung-Ho Kim*

Department of Biological Chemistry, College of Pharmacy, Chosun University, 375 Seosuk-dong, Dong-gu, Gwangju 501-759, South Korea

Received 5 June 2002; received in revised form 7 February 2003; accepted 10 February 2003

Abstract

Liver specific polymeric nanoparticles were designed and synthesized from biotinylated poly(ethylene glycol) conjugated with lactobionic acid containing a galactose moiety (abbreviated as BEL). Synthesized BEL conjugate was identified by Fourier transform-infrared (FT-IR) and ^{1}H-nuclear magnetic resonance (NMR) spectroscopy. The fluorescence spectroscopy data showed that BEL conjugate was self-assembled in water to form core-shell structure nanoparticles, and the critical association concentration (CAC) value was estimated as 0.028 g/l. From the transmission electron microscope (TEM) observation, the BEL nanoparticles were spherically shaped and ranged in size between 30 and 60 nm. The particle size distribution was measured by photon correlation spectroscopy (PCS), and the result was 41.2 ± 11.7 nm. Anti-cancer drug all-*trans*-retinoic acid (ATRA) was loaded into the BEL nanoparticles for evaluating its efficacy as a drug delivery carrier. The crystallinities of ATRA and ATRA-loaded nanoparticles were examined by X-ray diffraction (XRD) patterns. The ATRA release kinetics from the BEL nanoparticles showed a pseudo zero-order pattern during 1-month period.

Keywords: Polymeric nanoparticle; Biotin; Poly(ethylene glycol); Lactobionic acid; All-*trans*-retinoic acid

1. Introduction

Nanoparticles are colloidal particles of a size below 1 μm, and widely employed in various fields of life sciences, such as separation technologies, histological studies, clinical diagnostic assays, and drug delivery system (DDS). In the DDS applications, nanoparticles have several merits, like ease purification and sterilization, drug targeting possibility, and a sustained release action (Allemann et al., 1993). We synthesized various core-shell structure nanoparticles in our previous studies (Kim et al., 2000; Kim and Kim, 2001, 2002). Core-shell structure nanoparticles present advantages in regard of a long circulation in the body, drug solubility, drug stability, and relatively high level of hydrophobic drug encapsulation into the hydrophobic core (Gref et al., 1994; Peracchia et al., 1997; Yokoyama et al., 1990, 1991; Kwon et al., 1995).

Tissue-specific molecular delivery has been a valuable technique for biological medical research and for the diagnosis and cancer therapy. To achieve this goal, there needs to be an approach that can enable the chemical modification of carriers to allow the attachment of targeting ligands. The recognition of

* Corresponding author. Tel.: +82-62-230-6379; fax: +82-62-222-5414.
E-mail address: shkim@chosun.ac.kr (S.-H. Kim).

0378-5173/03/$ – see front matter
doi:10.1016/S0378-5173(03)00128-5

ligands on the surface of delivery systems by organ-specific or cell-specific receptors may result in the organ-targeted drug delivery (Takakura and Hashida, 1996; Daemen et al., 1988), or in improved drug uptake through ligand-induced endocytosis (Sato et al., 1996; Brown and Goldstein, 1986). In recent years, there has been growing interest in the area of liver cell-specific DDS. A great deal of effort has been made to achieve an appropriate liver targeting of chemotherapeutic agents with liposomes (Kim and Han, 1995), microspheres (Kim et al., 1993), and drug-carrier molecule conjugates (Seymour et al., 1991). Among the liver-associated surface receptors, the asialoglycoprotein receptor (ASGP-R: galactose receptor) is well known to be present on hepatocytes (Ashwell and Harford, 1982). It is also retained on several human hepatoma cell lines (Ciechanover et al., 1983). If a ligand binds to a galactose receptor, the ligand-receptor complex is rapidly internalized and the receptor recycles back to the surface (Nishikawa et al., 1993). Therefore, designing a DDS for galactose receptor-mediated endocytosis would be useful for targeting the hepatocyte/liver and hepatoma cells (Goto et al., 1994). The biotin content of cancerous tumors is higher than that of normal tissue. So, we expected that the biotin and the galactose moiety of the lactobionic acid could target together to the tumor cells in the liver. Biotin is a 244 Da, water-soluble vitamin (Vitamin H) composed of a 'head', represented by a complex aliphatic heterocycle, and an aliphatic 'tail', ending with a carboxyl group. The 'head' provides the most important contribution to the binding of biotin to avidin, while the carboxyl group can be rendered capable of reacting with several different functional groups (Elo and Korpela, 1984). To this carboxyl group, we conjugated the one terminal amino group of diamine-terminated poly(ethylene glycol) (PEG). And, subsequently the other amino group was coupled with the carboxyl group of lactobionic acid with galactose moiety. With this galactose moiety, it can be expected that the BEL nanoparticles are endocytosed by liver cells within several minutes, suggesting its preferential uptake mediated by asialoglycoprotein (ASGP) receptor as previous report (Hashida et al., 1995).

Retinoids have been shown to have substantial anticancer activity in a number of preclinical and clinical situations. All-*trans*-retinoic acid (ATRA), an active metabolite of retinol (Vitamin A) was chosen as a model anti-cancer drug. ATRA plays essential roles in the regulation of differentiation and proliferation of various cell types. It has been proved that ATRA is effective in the treatments of epithelial and hematologic malignancies such as head and neck cancer, lung cancer, breast cancer, ovarian adenocarcinoma, and acute promyelocytic leukemia (Han and Choi, 1996; Sccks et al., 1995; Trump et al., 1997).

In the present study, we prepared polymeric conjugate nanoparticles composed of biotin and diamine-terminated poly(ethylene glycol) with a galactose moiety from lactobionic acid. The polymeric conjugate (abbreviated as BEL) was physico-chemically characterized by FT-IR spectroscopy, fluorescence spectroscopy, PCS, and TEM. Anti-cancer agent ATRA loading was confirmed by XRD, and the release was studied in vitro to evaluate the possibility for DDS.

2. Materials and methods

2.1. Materials

Biotin, lactobionic acid (LA) and *N*,*N*′-dicyclohexyl carbodiimide (DCC) were purchased from the Aldrich Chemical Company (Milwaukee, WI). Diamine-terminated poly(ethylene glycol) (ATPEG) with a number-average molecular weight of 2000 was supplied by Texaco Chem. Co. (Ballaire, TX). *N*-Hydroxysuccinimide (NHS) was purchased from Sigma Chemical Co. (St. Louis, MO). Dialysis membrane with a molecular weight cutoff (MWCO) of 2000 g/mol was obtained from Spectra/Por^{TM} membranes. Dimethylsulfoxide (DMSO) and other chemicals were of reagent grade and used without further purification.

2.2. Synthesis of the BEL conjugate

The BEL conjugate was prepared by a two-step coupling reaction of biotin, ATPEG, and LA. First, the conjugation between biotin and one terminal of ATPEG was performed. Biotin (0.2 mmol) was dissolved in slightly heated water, DCC (0.4 mmol), NHS (0.4 mmol), and ATPEG (0.2 mmol) were separately dissolved in DMSO. The DCC/DMSO solution was added to the biotin solution, and stirred for

30 min to activate the carboxyl group of the biotin. The NHS/DMSO solution was added to the activated biotin solution, and the reactions were conducted at room temperature for 12 h. In the reaction mixture, dicyclohexylurea (DCU) was formed, so it was filtered to remove DCU. The ATPEG/DMSO solution was then added into the reaction mixture, and stirred for 30 min to complete the conjugation of activated biotin and ATPEG. The solution was placed in a dialysis membrane and dialyzed against distilled water for 7 days. The resultant solution in dialysis membrane was freeze-dried, and second conjugation between LA and the biotin/ATPEG (abbreviated as BE) conjugate was carried out in DMSO using the same procedure as mentioned above. Briefly, the LA, DCC, NHS, and BE were separately dissolved in DMSO. The carboxyl group of the LA was activated using DCC and NHS. After filtering the reaction mixture, BE was conjugated with the activated LA to obtain the BEL conjugate. The reaction solution was dialyzed for 7 days and freeze-dried. The freeze-dried BEL conjugate was stored in a refrigerator at 4 °C until use.

2.3. Characterization of BEL conjugate

FT-IR spectroscopy (Magna IR 550, Nicolet) was used to confirm the synthesis of BE and BEL conjugate. ^{1}H-NMR spectra were measured in DMSO-*d6* to confirm the synthesis of the BEL conjugate using a 300 MHz NMR spectrometer (Jeol, Japan).

2.4. Fluorescence spectroscopy

The BEL conjugate suspension was prepared as follows: 20 mg of the BEL conjugate was dissolved in 5 ml of DMSO and dialyzed using a dialysis membrane against distilled water for 2 days. The resulting solution in the dialysis membrane was adjusted to various concentrations of the BEL conjugate. The critical association concentration (CAC) of the BEL conjugate was estimated to prove the potential of nanoparticle formation by a spectrofluorophotometer (Shimadzu RF-5301 PC, Japan) using pyrene as a hydrophobic probe (Wilhelm et al., 1991; Kim et al., 2000; Kim and Kim, 2001, 2002). A known amount of pyrene in acetone was added to each of a series of 20 ml vials and the acetone was evaporated. The pyrene was then adjusted to give a final concentration of 6.0×10^{-7} M in 10 ml of various concentrations of conjugate suspension. The resultant suspensions were heated for 3 h at 65 °C to equilibrate pyrene and nanoparticles, and then left to cool overnight at room temperature. The emission wavelength used for the excitation spectra was 390 nm. The excitation and emission bandwidths were 1.5 and 1.5 nm, respectively.

2.5. TEM and PCS measurements

The morphology of the BEL nanoparticles was observed using a JEM-2000 FX II (Jeol, Japan) at 80 kV. A drop of polymeric nanoparticle suspension in water was placed on a copper grid coated with carbon film and dried at 20 °C. The specimen on the copper grid was negatively stained with 0.01% phosphotungstic acid. PCS was measured with a Zetasizer 3000 (Malvern Instruments, England) with a He–Ne laser beam at a wavelength of 633 nm at 25 °C at a scattering angle of 90°. The nanoparticle suspension was prepared by the diafiltration method, and the particle size was measured without filtering (concentration: 1 g/l).

2.6. Drug loading and in vitro drug release studies

The BEL conjugate (40 mg) was dissolved in 10 ml of DMSO and 10 mg of ATRA were added. The solution was stirred at room temperature and dialyzed against distilled water for 3 days using a dialysis membrane. For the measurement of drug-loading content, freeze-dried sample was suspended in dichloromethane by vigorous stirring for 2 h and then sonicated for 5 min. The resulting solution was centrifuged at 3000 rpm for 20 min, and the supernatant was analyzed using UV spectrophotometer (Shimadzu UV-1201, Japan) at 365 nm.

ATRA loading into the core portion of the BEL nanoparticles was verified by X-ray diffraction (XRD) measurement with a Rigaku D/Max-1200 (Rigaku) using Ni-filtered Cu Ka radiation (35 kV, 15 mA).

Five milligram of the ATRA-loaded BEL core-shell type nanoparticles were suspended in 1 ml PBS (phosphate buffer solution, pH 7.4) and subsequently placed into a dialysis membrane for release experiments. The dialysis membrane was placed into a 20 ml bottle with 10 ml PBS and the medium was stirred at 100 rpm at

37 °C. At set time intervals, the whole medium (10 ml) was taken and replaced with the same volume of fresh PBS. The concentration of the ATRA released in the PBS was determined by a UV spectrophotometer at 365 nm. All procedures were carried out in the dark because of the light-sensitivity of ATRA.

3. Results and discussion

The BEL conjugate was synthesized by two-step coupling with biotin, ATPEG, and LA. Synthesized BEL conjugate was confirmed by FT-IR and ^{1}H-NMR spectroscopy as shown in Figs. 1 and 2. The characte-

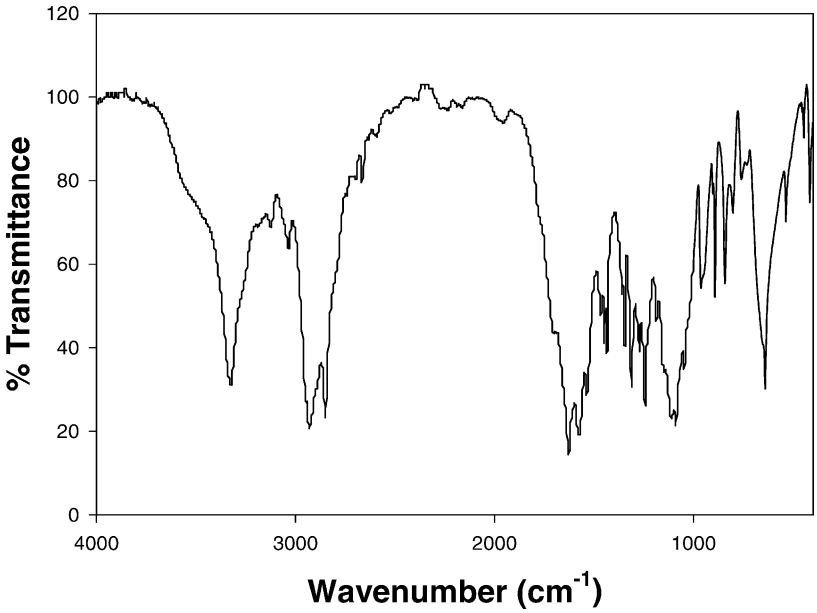

Fig. 1. FT-IR spectrum of the BEL conjugate.

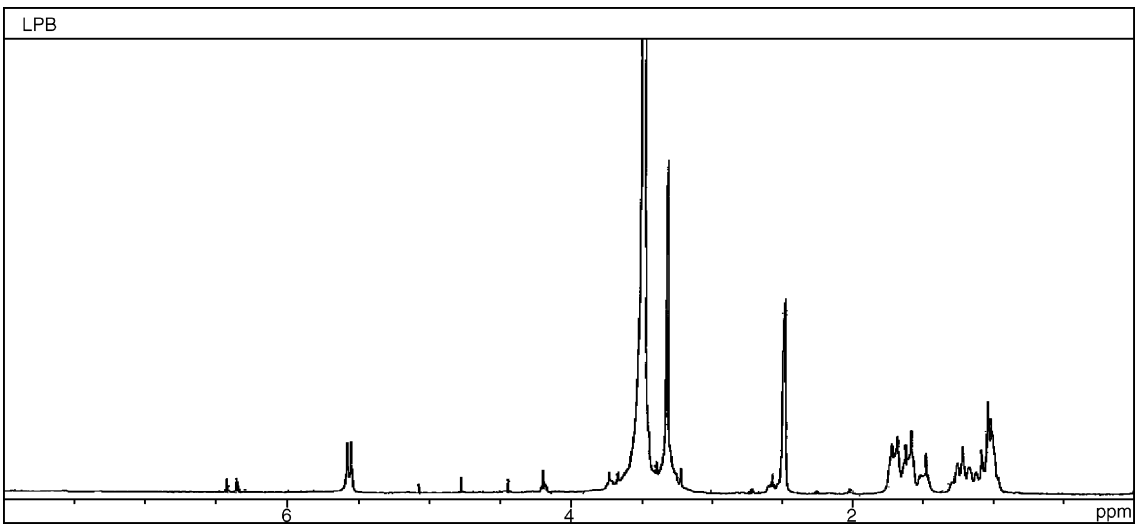

Fig. 2. ^{1}H-NMR spectrum of the BEL conjugate.

Table 1
Characteristic peaks assigned on the FT-IR spectra

Wavenumber (cm^{-1})	Assignments
3330	$–NH_2$
2920	$–CH_3$
2850	$–CH_2–$
1640	–C=O (amide)
1570	$–NH_2$

ristic peaks of FT-IR were listed in Table 1. Especially, two characteristic peaks on this spectrum, i.e. amide stretch absorption at 3330 cm^{-1}, and amide bending at 1570 cm^{-1}, may be used to verify the BEL conjugate. In Fig. 2, the proton signal of biotin appeared at approximately 3.3 ppm, the proton signal of LA was observed at 4.2 ppm, and the ethylene oxide proton signal of the ATPEG was observed at nearly 3.7 ppm.

From the previous studies, we certainly identified the nanoparticle formation of some amphiphilic conjugates (Kim et al., 2000; Kim and Kim, 2001, 2002). By the fluorescence technique using pyrene as a hydrophobic probe, the critical association concentration (CAC) was determined from the fluorescence emission and excitation spectra as pyrene partitions between aqueous and nanoparticular environments.

We measured the emission and excitation spectra of BEL conjugate using pyrene as a hydrophobic probe, and the fluorescence spectroscopy data showed the nanoparticle formation of the BEL conjugate as shown in Figs. 3 and 4. In Fig. 3, the fluorescence emission spectra of pyrene were shown against various BEL concentrations at a fixed excitation wavelength of 339 nm. The intensity of fluorescence increased with increasing BEL concentrations, which indicated the formation of self-assembled polymeric BEL nanoparticles in water. Fig. 4(a) represents the fluorescence excitation spectra of pyrene at various BEL conjugate concentrations. Pyrene excitation spectra were red-shifted by increasing BEL concentration. It is thought that pyrene is preferentially partitioned into the less polar microdomains of the hydrophobic core portion of the nanoparticles, since pyrene in a polar environment shows only weak fluorescence intensity. The (0,0) bands in the pyrene excitation spectra were examined and compared with the intensity ratio I_{336}/I_{334}; this ratio takes the characteristic value of pyrene in water at low concentrations and the value

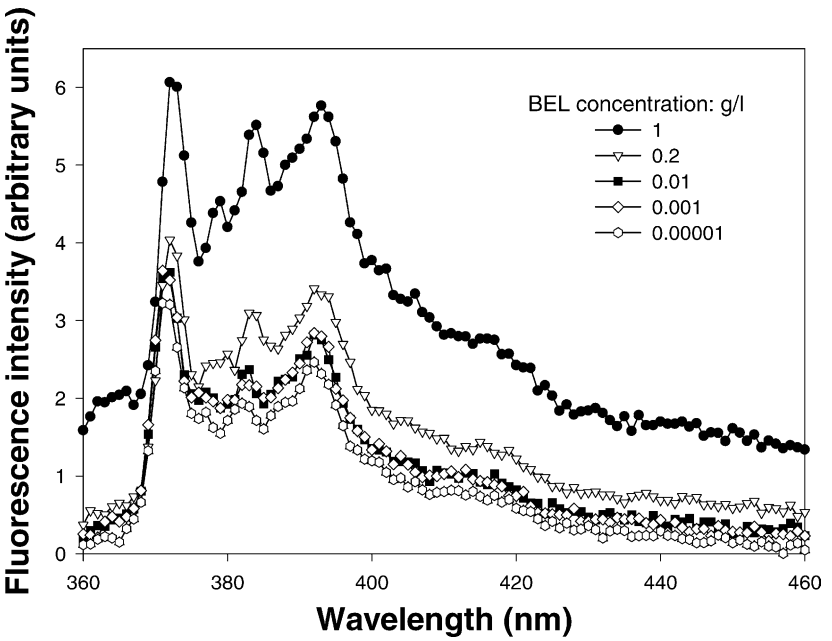

Fig. 3. Fluorescence emission spectra of pyrene/BEL against concentration of BEL in distilled water (excitation wavelength: 339 nm). [Pyrene] = 6.0×10^{-7} M.

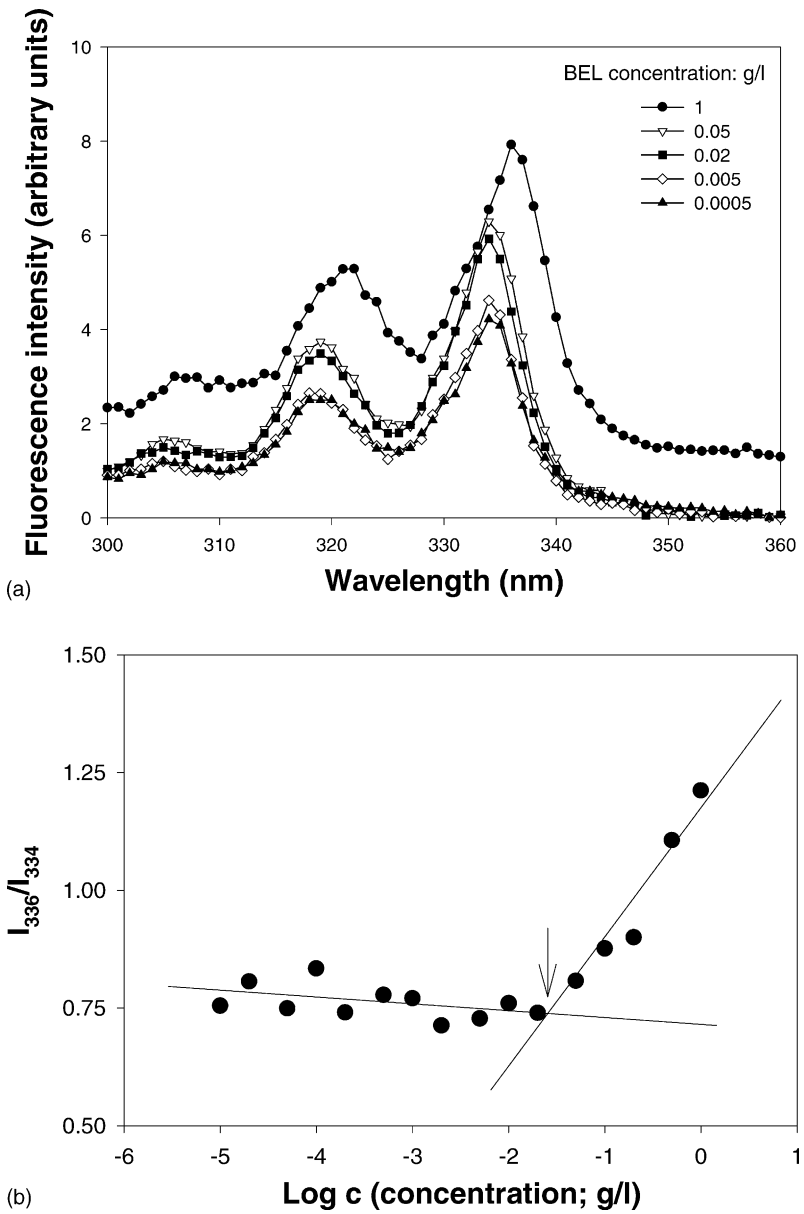

Fig. 4. Fluorescence excitation spectra of pyrene/BEL against concentration of BEL in distilled water (emission wavelength: 390 nm) (a) and plots of the intensity ratio I_{336}/I_{334} from pyrene excitation spectra vs. log C of the BEL conjugate in distilled water (b). [Pyrene] $= 6.0 \times 10^{-7}$ M.

of pyrene entirely in the hydrophobic domain. The fluorescence intensity ratios of I_{336}/I_{334} against the polymer concentration in the pyrene excitation spectra are plotted in Fig. 4(b) to a sigmoidal curve. The ratio is almost flat at low concentrations and rapidly increases at higher concentrations. The CAC value, which is the threshold concentration of self-aggregate formation by intra- and/or intermolecular association, was taken from the intersection of the tangent to the curve at the inflection with the horizontal tangent through

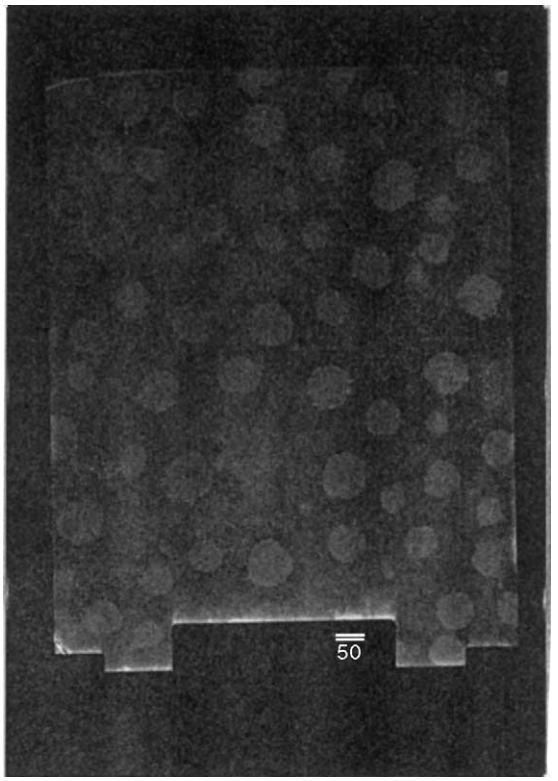

Fig. 5. TEM photograph of the BEL nanoparticles.

the lower concentration points. The estimated CAC was 0.028 g/l.

The morphological structures of the BEL nanoparticles are shown in Fig. 5. They appear negatively stained and spherical with sizes ranging from about 30 to 60 nm by TEM observation. The particle size distribution measured by PCS was 41.2 ± 11.7 nm coincide with the result of TEM.

Fig. 6 shows the incorporation of drug by XRD patterns of the drug only, empty and ATRA-loaded BEL nanoparticles. ATRA showed the sharp peaks of drug crystals, but the specific drug crystal peaks were reduced when the ATRA was entrapped into the BEL nanoparticles.

The calculated ATRA loading content was 36.2 wt.%. To investigate the release kinetics of the ATRA-loaded BEL nanoparticles were dispersed in a dialysis membrane containing PBS (0.1 M, pH 7.4). The total amounts of drug release from the BEL nanoparticles were detected by UV spectrophotometer at 365 nm at each time point. Fig. 7 shows that the hydrophobic ATRA can be released from the BEL nanoparticles with pseudo zero-order kinetics over 1-month period. It can be expected that the ATRA crystallize in the core portion of the BEL nanoparticles, so the crystallized drug is dissolved and diffused slowly into the outer aqueous phase relative to the molecular dispersion. In addition, the release kinetics of the hydrophobic drug can be controlled by the

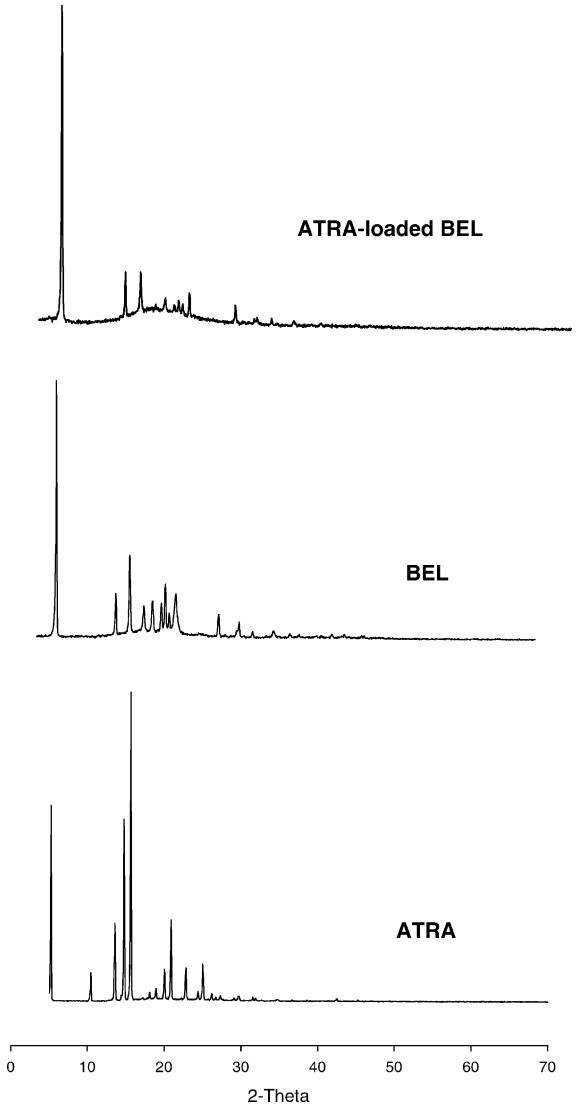

Fig. 6. XRD patterns of the ATRA, BEL, and ATRA-loaded BEL nanoparticles.

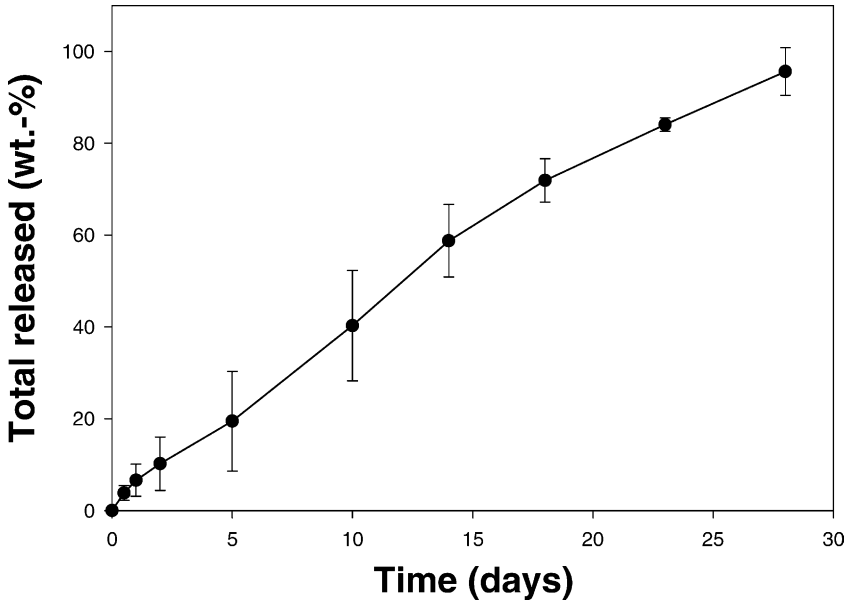

Fig. 7. ATRA release from the BEL nanoparticles ($n = 6$, mean ± S.D.).

loading content of drug inside of the nanoparticles (Jeong et al., 1998).

In conclusion, the BEL conjugate was successfully synthesized and characterized the physico-chemical properties. The hydrophobic drug ATRA was physically entrapped within the core of the BEL nanoparticles, and released with pseudo zero-order kinetics. The biotin combines tightly with the protein avidin, and it is expected that the BEL nanoparticles allow the co-delivery of certain drugs into the hepatic cancer cells by the specific complex formation of biotin in the BEL and avidin.

Acknowledgements

This work was supported by Korea Research Foundation Grant (KRF-2001-015-FP0127).

References

Allemann, E., Gurny, R., Doelker, E., 1993. Drug-loaded nanoparticles preparation method and drug targeting tissues. Eur. J. Pharm. Biopharm. 39, 173–191.

Ashwell, G., Harford, J., 1982. Carbohydrate-specific receptors of the liver. Annu. Rev. Biochem. 51, 531–554.

Brown, M.S., Goldstein, J.L., 1986. A receptor-mediated pathway for cholesterol homeostasis. Science 232, 34–47.

Ciechanover, A., Schwartz, A.L., Lodish, H.F., 1983. Sorting and recycling cell surface receptors and endocytosed ligands: the asialoglycoprotein and transferring receptors. J. Cell. Biochem. 23, 107–130.

Daemen, M.J., Smits, J.F., Thijssen, H.H., Struyker-Boudier, H.A., 1988. Pharmacokinetic consideration in target-organ directed drug delivery. Trends Pharm. Sci. 9, 138–141.

Elo, H.A., Korpela, J., 1984. The occurrence and production of avidin: a new conception of the high-affinity biotin-binding protein (review). Comp. Biochem. Physiol. B 78, 15–20.

Goto, M., Yura, H., Chang, C.W., Kobayashi, A., Shinoda, T., Maeda, A., Kojima, S., Kobayashi, K., Akaike, T., 1994. Lactose-carrying polystyrene as a drug carrier: investigation of body distribution to parenchymal liver cells using ^{125}I-labelled lactose-carrying polystyrene. J. Control. Release 28, 223–233.

Gref, R., Minamitake, Y., Peracchia, M.T., Trubetskoy, V., Torchilin, V., Langer, R., 1994. Biodegradable long-circulating polymeric nanospheres. Science 263, 1600–1603.

Han, S., Choi, J.H., 1996. Highly specific cytochrome P450-like enzyme for all-*trans* retinoic acid in T47D human breast cancer cells. J. Clin. Endocrinol. Metab. 81, 1–7.

Hashida, M., Nishikawa, M., Takakura, Y., 1995. Hepatic targeting of drugs and proteins by chemical modification. J. Control. Release 36, 99–107.

Jeong, Y.I., Cheon, J.B., Kim, S.H., Han, J.W., Lee, Y.M., Sung, Y.K., Akaike, T., Cho, C.S., 1998. Clonazepam release from core-shell type nanoparticles in vitro. J. Control. Release 51, 169–178.

Kim, C.K., Han, J.H., 1995. Lymphatic delivery and pharmacokinetics of methotrexate after intramuscular injection of

differently charged liposome-entrapped methotrexate to rats. J. Microencapsul. 12, 437–446.

Kim, C.K., Hwang, S.J., Lee, M.G., 1993. The organ targetability of small and large albumin microspheres containing free and HAS conjugate methotrexate. Int. J. Pharm. 89, 91–102.

Kim, I.S., Jeong, Y.I., Cho, C.S., Kim, S.H., 2000. Core-shell type polymeric nanoparticles composed of poly(L-lactic acid) and poly(*N*-isopropylacrylamide). Int. J. Pharm. 211, 1–8.

Kim, I.S., Kim, S.H., 2001. Evaluation of polymeric nanoparticles composed of cholic acid and methoxy poly(ethylene glycol). Int. J. Pharm. 226, 23–29.

Kim, I.S., Kim, S.H., 2002. Development of a polymeric nanoparticulate drug delivery system. In vitro characterization of nanoparticles based on sugar-containing conjugates. Int. J. Pharm. 245, 67–73.

Kwon, G.S., Naito, M., Yokoyama, M., Okano, T., Sakurai, Y., Kataoka, K., 1995. Physical entrapment of adriamycin in AB block copolymer micelles. Pharm. Res. 12, 192–195.

Nishikawa, M., Kamijo, A., Fujita, T., Takakura, Y., Sezaki, H., Hashida, M., 1993. Synthesis and pharmacokinetics of a new liver-specific carrier, glycosylated carboxymethyl-dextran, and its application to drug targeting. Pharm. Res. 10, 1253–1261.

Peracchia, M.T., Gref, R., Minamitake, Y., Domb, A., Lotan, N., Langer, R., 1997. PEG-coated nanospheres from amphiphilic diblock and multiblock copolymers: investigation of their drug encapsulation and release characteristics. J. Control. Release 46, 223–231.

Sato, J., Sugiyama, Y., Tsuji, A., Horikoshi, I., 1996. Importance of receptor-mediated endocytosis in peptide delivery and targeting: kinetic aspects. Adv. Drug Deliv. Rev. 19, 445–467.

Sccks, P.G., Harris, D., Chou, T.C., 1995. Modulation of growth and proliferation in squamous cell carcinoma by terinoic acid: a rationale for combination therapy with chemotherapeutic agents. Int. J. Cancer 61, 409–415.

Seymour, L.W., Ulbrich, K., Wedge, S.R., Hume, I.C., Strohalm, J., Duncan, R., 1991. *N*-(2-Hydroxypropyl)methacrylamide copolymer targeted to the hepatocyte galactose-receptor: pharmacokinetics in DBA2 mice. Br. J. Cancer 63, 859–866.

Takakura, Y., Hashida, M., 1996. Macromolecular carrier systems for targeted drug delivery: pharmacokinetic considerations on biodistribution. Pharm. Res. 13, 820–831.

Trump, D.L., Smith, D.C., Stiff, D., Adedoyin, A., Day, R., Bahnson, R.R., Hofacker, J., Branch, R.A., 1997. A phase II trial of all-trans-retinoic acid in hormone-refractory prostate cancer: a clinical trial with detailed pharmacokinetic analysis. Cancer Chemo-Ther. Pharmacol. 39, 349–356.

Wilhelm, M., Zhao, C.L., Wang, Y., Xu, R., Winnik, M.A., Mura, J.L., Riess, G., Croucher, M.D., 1991. Poly(styrene-ethylene oxide) block copolymer micelle formation in water: a fluorescence probe study. Macromolecules 24, 1033–1040.

Yokoyama, M., Miyauchi, M., Yamada, N., Okano, T., Sakurai, Y., Kataoka, K., Inoue, S., 1990. Characterization and anticancer activity of micelle-forming polymeric anticancer drug adryamycin—conjugated poly(ethylene glycol)-poly(asparatic acid) block copolymer. Cancer Res. 50, 1693–1970.

Yokoyama, M., Okano, T., Sakurai, Y., Ekimoto, H., Shibazaki, C., Kataoka, K., 1991. Toxicity and antitumor activity against solid tumors of micelle-forming polymeric anticancer drug and its extremely long circulation in blood. Cancer Res. 51, 3229–3236.